

Solar Energy to Drive Half-Effect Absorption Cooling System

Rabah GOMRI *

*Laboratory of Génie Climatique, Engineering Faculty, Department of Génie Climatique
25000, Constantine, Algeria*

Abstract

This paper presents the simulation results and an overview of the performance of low capacity two stage half-effect absorption cooling system (10kW), suitable for residential and small building applications. The primary heat source is solar energy supplied from flat plate collectors. The complete system (solar collectors-absorption cooling system) was simulated using a developed software program. The energy and exergy analysis is carried out for each component of the system. All exergy destructed that exist in this solar cooling system is calculated. Critical temperatures which are the minimum allowable hot water inlet temperatures are determined. This system has shown promising characteristics. When the condenser temperature is fixed at 28°C, 32°C and 36°C it can be concluded that between time of day 10 and 14 solar collector provides about 96%, 95% and 91% heating energy required respectively with a cover of about 100% between time of day 11 and 13 which correspond to a maximum of solar radiation. The daily cover is about 71%, 70% and 65% respectively.

Keywords: *Absorption cooling system; Performance; Solar energy; Two stage; Half-effect system.*

1. Introduction

Nowadays world is marked with an intensive use of energy, cooling and air conditioning remains having the large share of energy consumption. Besides the energy consumption, climatic changes have become an international issue that was treated in many international summits (the last one was the United Nations Climate Change Conference Copenhagen – December 2009). In this context, solar chilled water production through absorption cycles energy may be considered one of the most desirable applications to reduce energy consumption and CO₂ gas emissions. The use of solar energy to drive cooling cycles for air conditioning is an attractive concept because of the coincidence of peak cooling loads with the available solar power.

Algeria, as well as most of other Arab countries, enjoys of solar radiations. During the summer, the demand for electricity greatly increases because of the use of vapour compression air conditioning system, which increases the peak electric load, and major problems in the country's electric supply arise. Solar energy can be used for cooling as it can assist in providing the heating energy for absorption cooling systems.

Two types of the absorption chillers, the single effect and half effect cycles, can operate using low temperature hot water. By using a two stage half-effect LiBr absorption chiller instead of single effect chiller, it is possible to decrease the required generator temperature of the chiller and this allowed the use of simple flat plate collectors to produce hot water to be used as the hot source for absorption chiller.

The principle of the half-effect cycle is that it has two lifts. The term lift is used to represent a concentration difference between the generator and absorber. This concentration difference is what drives or gives the potential for mass to flow into the absorber. With the single effect there is only one lift. Many researchers have reported works on half-effect cycles. Ma and Deng [1] have reported preliminary results of an experimental investigation on a 6 kW vapour absorption system working on half-effect cycle with H₂O-LiBr as the working fluids. With hot water temperature requirement of around 85°C, a chilled water temperature of 7°C has been reached in their experiment. Sumathy et al. [2] have tested solar cooling and heating system with a 100 kW half-effect absorption chiller working on the same cycle. The system has been used successfully with generation temperatures in the range of 65–75°C to achieve a chilled water temperature of 9°C. Arivazhagan et al. [3] presented a simulation studies conducted on a half-effect vapour absorption pair cycle using R134a-DMAC as the refrigerant-absorbent pair with low

* Corresponding author. Tel.: +664317045

Fax: +9876543210; E-mail: rabahgomri@yahoo.fr

© 2010 International Association for Sharing Knowledge and Sustainability

DOI: 10.5383/ijtee.01.01.001

temperature heat sources for cold storage applications. Arivazhagan et al. [4] presented experimental studies on the performance of a two-stage half effect vapour absorption cooling system. The prototype was designed for 1 kW cooling capacity using HFC based working fluids (R134a as refrigerant and DMAC as absorbent).

In the paper presently considered, it is planned to use solar two-stage half-effect vapour absorption cooling machine to produce chilled water for air conditioning. This study aims at assessing the feasibility of solar powered absorption cooling systems under Algerian conditions. The system proposed to provide cooling in summer (June, July August and September) for a building located in Constantine, east of Algeria (longitude 6.62 °E, latitude 36.28°N and altitude of 689m). The results presented in this paper were for 1-day period operation (21st of July).

2. Simulation of the Performance

2.1. Solar collector system

The various relations that are required in order to determine the useful energy collected and interaction of the various structural parameters on the performance of a collector are taken from [5-10].

The energy balance equation of the solar collector can be written as follows [5]:

$$I_G \cdot A_c = Q_u + Q_{\text{loss}} + Q_{\text{stg}} \quad (1)$$

Where I_G is the instantaneous solar radiation incident on the collector per unit area, A_c is the collector surface area, Q_{loss} is the heat loss from the collector and Q_u is the useful energy transferred from the absorber to the fluid flowing through the tubes of the collector. Q_{stg} is the energy stored in the collector ($Q_{\text{stg}}=0$: the solar thermal system is considered at steady state conditions).

The useful energy gain of the flat plate collectors is calculated by:

$$Q_u = A_c \cdot F_R \cdot [(\tau \cdot \alpha) I_G - U_L \cdot (T_{\text{fi}} - T_a)] \quad (2)$$

Where A_c is the collector area, F_R is the collector heat removal factor, $(\tau \cdot \alpha)$ is the transmittance-absorptance products, U_L is the collector overall loss coefficient, T_a is the ambient air temperature and T_{fi} is the fluid temperature at the inlet to the collector.

The Collector heat removal factor (F_R) is the ratio of useful heat obtained in collector to the heat collected by collector when the absorber surface temperature is equal to fluid entire temperature on every point of the collector surface.

$$F_R = \frac{m \cdot C_p}{A_c \cdot U_L} \left[1 - e^{-\frac{(A_c \cdot U_L \cdot F')}{m \cdot C_p}} \right] \quad (3)$$

Where m is the mass flow rate of water, C_p is the specific heat of water and F' is the collector efficiency factor. F' represents the ratio of the actual useful energy gain to the useful energy gain that would result if the collector absorbing surface had been at local fluid temperature.

The collector overall heat loss coefficient (U_L) is the sum of the top (U_T , bottom U_B and edge U_E heat loss coefficient. It means that:

$$U_L = U_T + U_B + U_E \quad (4)$$

The first law efficiency (thermal efficiency) of the solar collectors is the ratio of useful energy obtained in collector to solar radiation incoming to collector. It can be formulated as:

$$\eta_{\text{th-FPC}} = \frac{Q_u}{I_G \cdot A_c} \quad (5)$$

The prediction of collector performance requires knowledge of the absorbed solar energy by collector absorber plate. The solar energy incident on a tilted collector consists of three different distributions: beam radiation, diffuse radiation, and ground – reflected radiation. The details of the calculation depend on which diffuse sky model is used. For estimating sky diffuse solar radiations several models have been developed [11-15]. They vary mainly in the ways that treat the three components of the sky diffuse radiation, i.e. the isotropic, circumsolar and horizon radiation streams. In this study the absorbed radiation on the absorber plate is calculated by Perez's model [16].

For the estimation of the ground reflected radiation an average value of the ground albedo of 0.2 is used.

2.2. Half-effect effect absorption cooling system

The two stage half-effect absorption refrigeration system as shown in Fig. 1 consists of condenser, evaporator, two generators, two absorbers, two pumps, two solution heat exchangers, two solution reducing valves and a refrigerant expansion valve. In the system operation, the evaporator and low pressure absorber operate at low pressure (evaporation pressure P_{ev}). The low pressure generator (LPG) and high absorber operate at intermediate pressure (P_1) and the high pressure generator (HPG) and the condenser operate at high pressure (condenser pressure, P_{cd}). Both generators (LPG and HPG) can be supplied with heat at the same temperature.

The refrigerant vapour from the evaporator is absorbed by the strong solution in the low absorber. The weak solution from the low absorber is pumped to the low generator through the low solution heat exchanger. The strong solution in the low generator is returned to the low absorber through the low solution heat exchanger. The refrigerant vapour from the low generator is absorbed by the strong solution in the high absorber. The weak solution from the high absorber is pumped to the high generator through the high solution heat exchanger. The strong solution in the high generator is returned to the high absorber through the high solution heat exchanger. In both heat exchangers, the weak solution from the absorber is heated by the strong solution from the generator. The refrigerant is boiled out of the solution in the high generator and circulated to the condenser. The liquid refrigerant from the condenser is returned to the evaporator through an expansion valve.

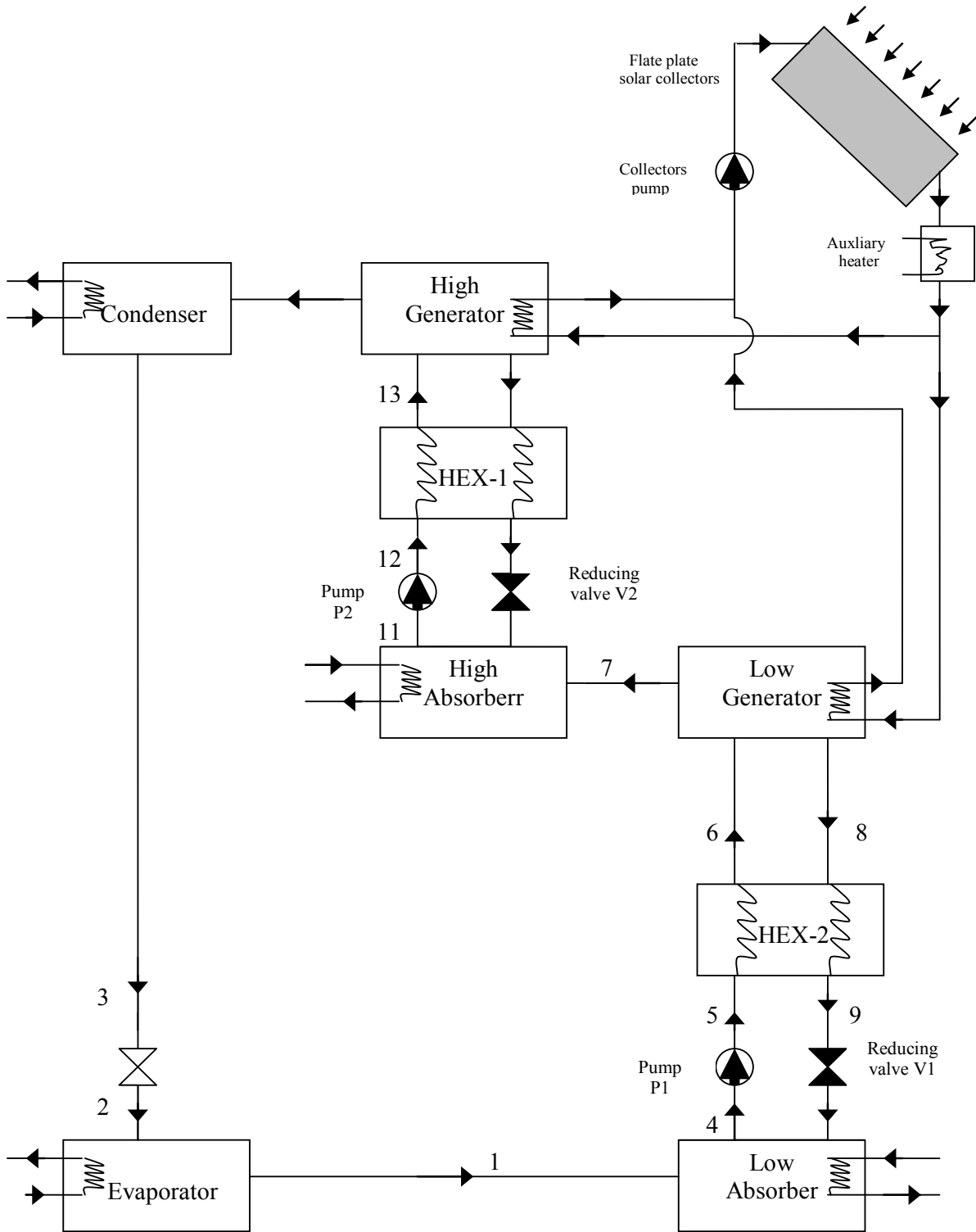


Fig. 1. The schematic illustration of solar two stage half-effect absorption cooling system

The half-effect effect absorption cooling system is simulated assuming the following conditions:

- The analysis is made under steady conditions.
- The refrigerant (water) at the outlet of the condenser is saturated liquid.
- The refrigerant (water) at the outlet of the evaporator is saturated vapour.
- The Lithium bromide solution at the absorber outlet is a strong solution and it is at the absorber temperature
- The outlet temperatures from the absorbers and from generators correspond to equilibrium conditions of the mixing and separation respectively.
- Pressure losses in the pipelines and all heat exchangers are negligible.

- Heat exchange between the system and surroundings, other than in that prescribed by heat transfer at the HPG, evaporator, condenser and absorber, does not occur
- The reference environmental state for the system is water at an environment temperature T_0 of 25°C and 1 atmospheric pressure (P_0)
- The system produce chilled water, and generators are driven by hot water.
- The system rejects heat to cooling water at the condenser and absorbers.
- Both generators are supplied with heat at the same temperature.
- The refrigerant flow rate leaving the low temperature generator is equal to the refrigerant flow rate leaving the high temperature generator.

Simulations are carried out for a constant refrigeration capacity $Q_{ev}=10kW$, Pump efficiency $\eta_p =85\%$, Heat exchangers effectiveness $\varepsilon_i=\varepsilon_{II}=70\%$, condensation temperature is equal to the absorber temperature $T_{cd}=T_{ab}$. Condensation temperature is varied in the following range: $T_{cd}=28^\circ C$ to $36^\circ C$. The outlet temperature of cooling water has been assumed at $T_{cd}-3$ and the inlet temperature of cooling water has been assumed at $T_{cd}-8$. Evaporation temperature is maintained at $T_{ev}=5^\circ C$. The outlet temperature of chilled water has been assumed at $T_{ev}+3$ and the inlet temperature of chilled water has been assumed at $T_{ev}+8$. Generation temperature “ T_g ” is varied from $42^\circ C$ to $62^\circ C$. The outlet temperature of hot water has been assumed at T_g+8 and the inlet temperature of hot water has been assumed at T_g+21 .

In this analysis, the thermal-physical properties of the working fluids have to be known as analytic functions. A set of computationally efficient formulations of thermodynamic properties of lithium bromide/water solution and liquid water developed by Patek and Klomfar [17] are used in this work. The equations for the thermal properties of steam are obtained from correlation provided by Patek and Klomfar [18].

For the thermodynamic analysis of the absorption system the principles of mass conservation and first law of thermodynamic are applied to each component of the system (see Fig. 1).

Mass Conservation: Mass conservation includes the mass balance of total mass and each material of the solution. The governing equations of mass and type of material conservation for a steady state and steady flow system are:

$$\sum m_i - \sum m_o = 0 \quad (6)$$

$$\sum m_i \cdot x_i - \sum m_o \cdot x_o = 0 \quad (7)$$

Where m is the mass flow rate and x is de mass fraction of LiBr in the solution. The mass fraction of the mixture at different points of the system (Fig.1) is calculated using the corresponding temperature and pressure data.

The mass flow rate of refrigerant is obtained by energy balance at evaporator and is given as,

$$m_3 = \frac{Q_{ev}}{(h_2 - h_3)} \quad (8)$$

Energy analysis: The first law of thermodynamics yields the energy balance of each component of the absorption cooling system as follows:

$$(\sum m_i \cdot h_i - \sum m_o \cdot h_o) + (\sum Q_i - \sum Q_o) + W = 0 \quad (9)$$

The thermal efficiency (coefficient of performance) of the absorption cooling system is obtained by

$$COP = \frac{Q_{ev}}{(Q_{HPG} + Q_{LPG} + W_{p1} + W_{p2})} \quad (10)$$

Exergy analysis: Exergy analysis is the combination of the first and second law of thermodynamics and is defined as the maximum amount of work, which can be produced by a stream or system as it is brought into equilibrium with a reference environment and can be thought of as a measure of the usefulness or quality of energy [19]. According to Bejan et al. [20] the exergetic balance applied to a fixed control volume is given by the following equation:

$$Ex_d = \left(\sum_i m_i \cdot ex_i \right)_{in} - \left(\sum_i m_i \cdot ex_i \right)_{out} - Ex_{heat j} - W \quad (11)$$

Where Ex_d is rate of exergy destruction. Ex_{heat} is the net exergy transfer by heat at temperature T , which is given by

$$Ex_{heat} = \sum_j \left(1 - \frac{T_0}{T_j} \right) \cdot Q_i \quad (12)$$

W is the mechanical work transfer to or from the system.

The specific exergy of flow is:

$$ex = (h - h_0) - T_0(s - s_0) \quad (13)$$

m is the mass flow rate of the fluid stream, h is the enthalpy, s is the entropy and the subscripts 0 stands for the restricted dead state.

The exergetic efficiency (rational efficiency) can be calculated as the ratio between the net exergy produced by the evaporator (exergy desired output) and the input exergy to the generator (exergy used) plus the mechanical work of the solution pumps:

$$\eta_{\text{exergy}} = \frac{Q_{\text{ev}} \cdot \left(1 - \frac{T_0}{T_b}\right)}{\left[(Q_{\text{gH}} + Q_{\text{gL}}) \left(1 - \frac{T_0}{T_h}\right) + (W_{\text{p1}} + W_{\text{p2}}) \right]} \quad (14)$$

T_b and T_h are the mean temperature of the cold source (in the evaporator) and the hot source (in the generator) respectively. Q_{gH} is the heat supplied to the HPG and Q_{gL} is the heat supplied to the LPG.

2.3. Mathematical model for the global system

For this part, the mathematical model is based on the following assumptions:

- The solar collector loop is chosen without a storage tank.
- An auxiliary heat source is provided, so that the hot water is supplied to generators when solar energy is not sufficient to heat the water to the required temperature level needed by the generators
- The overall thermal efficiency of the complete solar absorption cooling system η_{overall} is the product of COP and solar efficiency $\eta_{\text{th-FPC}}$ [21] :

$$\eta_{\text{overall}} = \text{COP} \cdot \eta_{\text{th-FPC}} \quad (15)$$

$$Q_{\text{gH}} + Q_{\text{gL}} = Q_u + Q_{\text{aux}} \quad (16)$$

Q_{aux} is the auxiliary heating load.

3. Results and Discussion

The energy and exergy analysis was carried out on 21st of July in Constantine (East of Algeria; Latitude 36.28°N, Longitude 6.62°E). A computer program was written for thermodynamic analysis. The program was based on the energy balance, exergy balance and thermodynamic properties for each reference point. The initial conditions are given into the program including the ambient conditions, the solar energy collector parameter specification, the component temperatures, pumps efficiencies, effectiveness of heat exchangers and evaporator load. With the given parameters, the thermodynamic properties at all reference points in the system were calculated. The results obtained from the present study may be presented as follows.

Fig. 2 shows the effects of the generator, and condenser temperature on the coefficient of performance (COP).

The high values of COP are obtained at high generator and low condenser temperatures. For a given evaporator and condenser temperature, there is a minimum generator temperature which corresponds to a maximum COP. It should be noted that the COP initially exhibits significant increase with an increase of generator temperature, and then the slope of the COP curves become almost flat. In other words, increasing the generator temperature higher than a certain value does not provide much improvement for the COP.

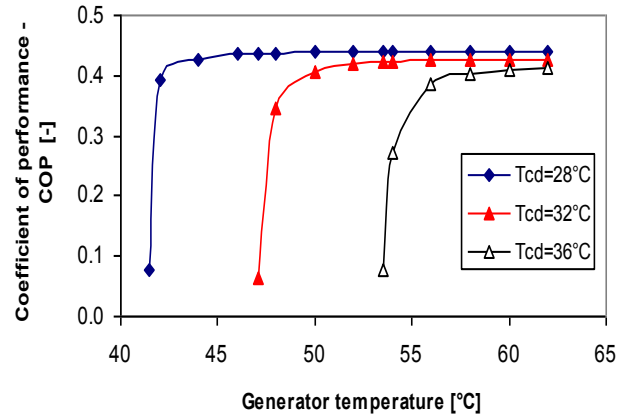


Fig.2. Coefficient of performance versus generator temperature 'Tg' and condenser temperature 'Tcd' (Tev=5°C)

The variation of exergetic efficiency with generator temperature for two stage half-effect cooling system at different condenser temperatures is shown in Fig. 3. Exergetic efficiency increase with an increase in the generator temperature up to a certain generator temperature (for a given evaporator, absorber and condenser temperature, there is a minimum generator temperature which corresponds to a maximum exergy efficiency) and then decrease.

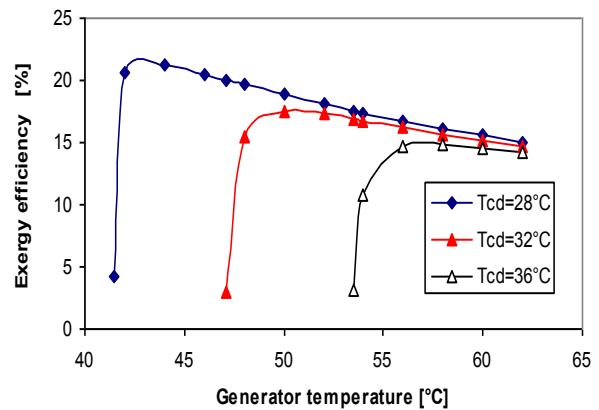


Fig.3. Exergy efficiency versus generator temperature 'Tg' and condenser temperature 'Tcd' (Tev=5°C)

The variation of total exergy loss with generator temperature for cooling at different condenser temperatures is shown in Fig. 4. The total exergy loss of the absorption cooling system drops sharply to a minimum value with an increase of generator temperature and then increases further. For each condenser temperature there is a generator temperature at which the total exergy loss of the absorption cooling system is minimum which corresponds to a maximum value of exergy efficiency and COP. In this study When the evaporator temperature is maintained constant at 5°C and condenser temperature is varied from 28°C and 36°C and generators temperatures are varied from 42 to 62 °C the maximum COP is 0.44 and the maximum exergetic efficiency is about 21%

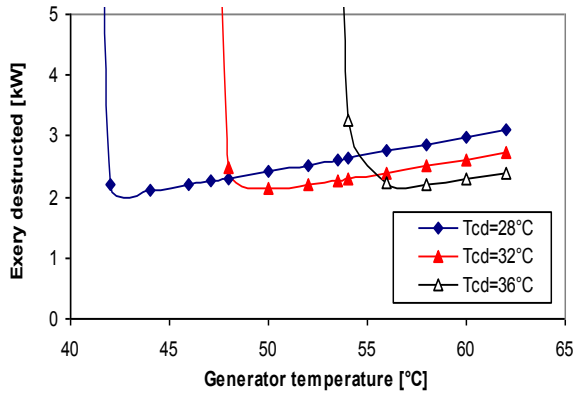


Fig.4. Exergy destroyed versus generator temperature 'Tg' and condenser temperature 'Tcd' (Tev=5°C)

Fig. 5 shows the variation of heat supplied to the two generators (Qg) versus the generator temperature for different value of condenser temperature. It is clear that for a given condenser temperature there is a minimum generator temperature for which the Qg is minimum. This optimum generator temperature corresponds to the generator temperature giving the maximum COP and exergetic efficiency of the absorption cooling system. It should be noted that the Qg initially exhibits a significant decrease with an increase of generator temperature, and then the slope of the Qg curves become almost flat. At higher generator temperature the values of Qg became almost the same for the different condenser temperatures.

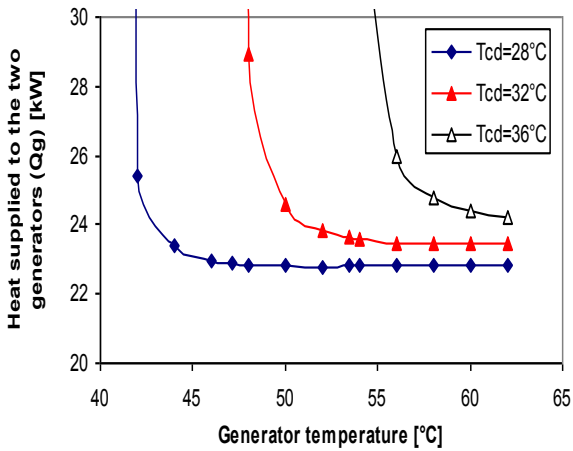


Fig.5. Heat supplied to the two generators versus generator temperature 'Tg' and condenser temperature 'Tcd' (Tev=5°C)

Fig. 6 shows the variation of the number of flat plate solar collector (N_{FPC}) during the peak solar gain hour on 21st of July versus the generator temperature for different value of condenser temperature. For a given condenser temperature there is an optimum generator temperature for which the N_{FPC} is minimum. This optimum generator temperature corresponds to the generator temperature giving the maximum COP and the maximum exergetic efficiency of the absorption cooling system.

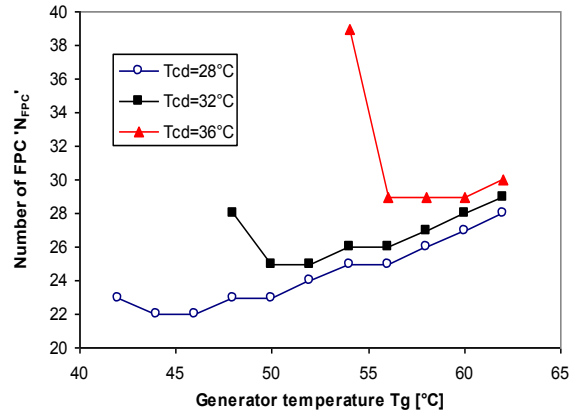


Fig.6. Variation of the number of FPC 'N_{FPC}' versus generator temperature 'Tg' and condenser temperature (Ac=2.03m²)

Figs. 7, 8 and 9 show the variation of energy efficiency of solar flat plate collectors (solar collector thermal efficiency, η_{th-FPC}), against time of day for different generator and condenser temperatures. It can be seen that the instantaneous collector efficiency is slightly higher after 12h and then decreases gradually at the shut off of operation hour. We note the existence of a maximum value of roughly 0.6 corresponding to the maximum incident radiation (also a minimum generator temperature of 42°C and a minimum condenser temperature of 28°C).

The COP of the absorption cooling system is a constant value during all the day then and as can be seen from "(Eq.1)" the thermal efficiency of the global system will decrease with an increase of the generator temperature and condenser temperature

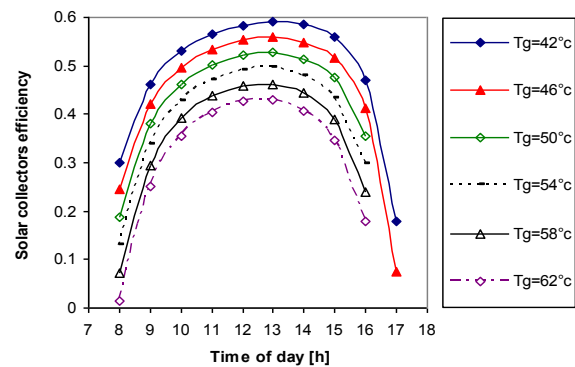


Fig.7. Variation solar collectors thermal efficiency versus time of day and generator temperature 'Tg' (Tcd=28°C)

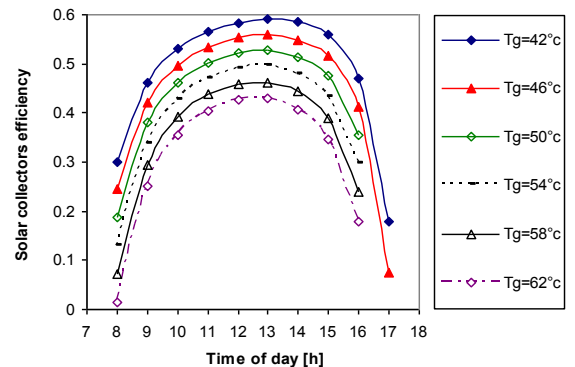


Fig.8. Variation solar collectors thermal efficiency versus time of day and generator temperature 'Tg' (Tcd=32°C)

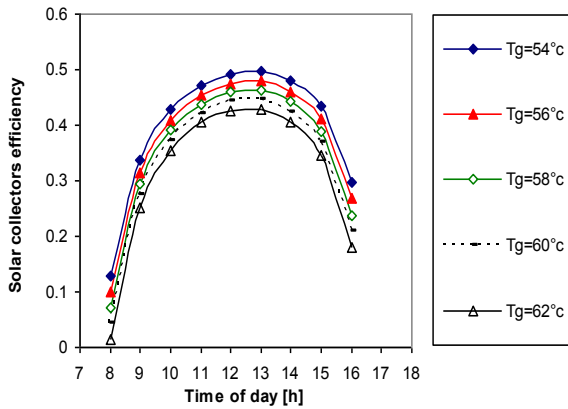


Fig.9. Variation solar collectors thermal efficiency versus time of day and generator temperature 'Tg' (Tcd=36°C)

Figs. 10, 11 and 12 show the variation of energy delivered to the two generators (LPG and HPG) and the contribution percentage of solar energy and auxiliary heating load. When the condenser temperature is fixed at 28°C, 32°C and 36°C it can be seen that between time of day 10 and 14 solar collector provides about 96%, 95% and 91% heating energy required respectively with a cover of about 100% between time of day 11 and 13 which correspond to a maximum of solar radiation. The daily cover is about 71%, 70% and 65% respectively. Then, a high value of condenser temperature influence negatively the rate of solar energy provided. The low solar radiation values early in the morning and later in the afternoon hours cause a significant increase in required auxiliary heating.

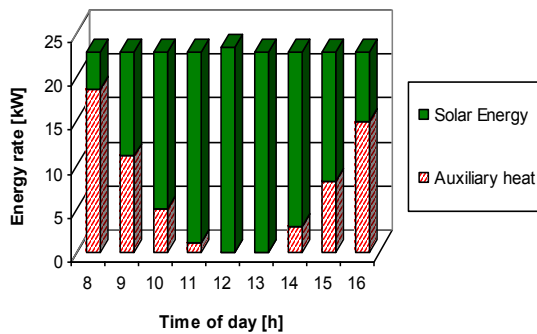


Fig. 10 Contribution percentage of solar energy and auxiliary heating load (Tcd=28°C, Tg=48°C)

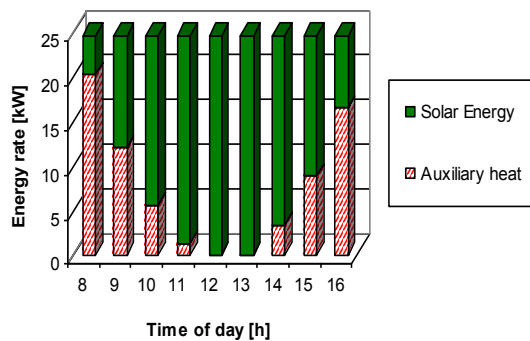


Fig. 11 Contribution percentage of solar energy and auxiliary heating load (Tcd=32°C, Tg=50°C)

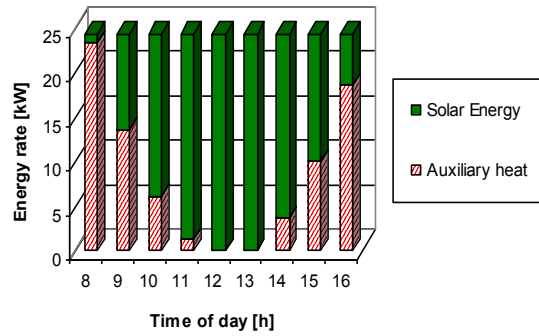


Fig. 12 Contribution percentage of solar energy and auxiliary heating load (Tcd=36°C, Tg=60°C)

3. Conclusion

In this paper, an attempt has been made to study the combination: flat plate solar collectors and a two stage absorption cooling system. The main results obtained are concluded below:

- When the evaporator temperature is maintained constant at 5°C and condenser temperature is varied from 28°C and 36°C and generators temperatures are varied from 42 to 62 °C the maximum COP is 0.44 and the maximum exergetic efficiency is about 21%
- For a given condenser temperature there is an optimum generator temperature for which the N_{FPC} is minimum. This optimum generator temperature corresponds to the generator temperature giving the maximum COP and exergetic efficiency of the absorption cooling system.
- We note the existence of a maximum value of solar collector thermal efficiency, η_{th-FPC} of roughly 0.6.
- The thermal efficiency of the global system will decrease with an increase of the generator temperature and condenser temperature

References

- [1] Ma WB, Deng SM. Theoretical analysis of low temperature hot source driven two stage LiBr-H₂O absorption refrigeration system. International Journal of refrigeration 1996; 19(2): 141-146. [http://dx.doi.org/10.1016/0140-7007\(95\)00054-2](http://dx.doi.org/10.1016/0140-7007(95)00054-2)
- [2] Sumathy K, Huang ZC, Li ZF. Solar absorption cooling with low grade heat source - A strategy of development in South China. Solar Energy 2000; 72 (2): 155-165. [http://dx.doi.org/10.1016/S0038-092X\(01\)00098-6](http://dx.doi.org/10.1016/S0038-092X(01)00098-6)
- [3] Arivazhagan S, Murugesan SN, Saravanan R, Renganarayanan S. Simulation studies on R134a-DMAC based half effect absorption cold storage systems. Energy Conversion and Management 2005;46(11-12):1703-1713. <http://dx.doi.org/10.1016/j.enconman.2004.10.006>
- [4] Arivazhagan S, Saravanan R, Renganarayanan R. Experimental studies on HFC based two-stage half effect vapour absorption cooling system. Applied Thermal Engineering 2006; 26 (14-15): 1455-1462. <http://dx.doi.org/10.1016/j.applthermaleng.2005.12.014>

- [5] Frederick FS. Flat plate solar collector performance evaluation with a solar simulator as a basis for collector selection and performance prediction. *Solar Energy* 1976; 18(5) : 451–466. [http://dx.doi.org/10.1016/0038-092X\(76\)90012-8](http://dx.doi.org/10.1016/0038-092X(76)90012-8)
- [6] Kalogirou SA. Solar thermal collectors and applications. *Progress in energy and combustion science* 2004;30(3): 231-295. <http://dx.doi.org/10.1016/j.peccs.2004.02.001>
- [7] Uca A, Inalli M. thermo-economical optimization of a domestic solar heating plant with seasonal storage. *Applied Thermal Engineering* 2007; 27 (2-3): 450–456. <http://dx.doi.org/10.1016/j.applthermaleng.2006.06.010>
- [8] Karatasou S, Santamouris M, Geros V. On the calculation of solar utilizability for south oriented flat plate collectors tilted to an angle equal to the local latitude. *Solar energy* 2006; 80(12):1600-1610. <http://dx.doi.org/10.1016/j.solener.2005.12.003>
- [9] Akhtara N, Mullick SC. Computation of glass-cover temperatures and top heat loss coefficient of flat-plate solar collectors with double glazing. *Energy* 2007; 32 (7): 1067-1074. <http://dx.doi.org/10.1016/j.energy.2006.07.007>
- [10] Sartori E. Convection coefficient equations for forced air flow over flat surfaces. *Solar Energy* 2006;80(9):1063–1071. <http://dx.doi.org/10.1016/j.solener.2005.11.001>
- [11] Bugler JW. The determination of hourly insolation on an inclined plane using a diffuse irradiance model based on hourly measured global horizontal insolation. *Solar Energy* 1977;19(5):477–491. [http://dx.doi.org/10.1016/0038-092X\(77\)90103-7](http://dx.doi.org/10.1016/0038-092X(77)90103-7)
- [12] Klucher T. Evaluation of models to predict insolation on tilted surfaces. *Solar Energy* 1979;23(2):111–114. [http://dx.doi.org/10.1016/0038-092X\(79\)90110-5](http://dx.doi.org/10.1016/0038-092X(79)90110-5)
- [13] Gueymard C. An isotropic solar irradiance model for tilted surfaces and its comparison with selected engineering algorithms. *Solar Energy* 1987; 38 (5): 367–386. [http://dx.doi.org/10.1016/0038-092X\(87\)90009-0](http://dx.doi.org/10.1016/0038-092X(87)90009-0)
- [14] Reindl DT, Beckman DA, Duffie JA. Evaluation of hourly tilted surface radiation models. *Solar Energy* 1990;45(1): 9–17, 1990.
- [15] Perez R, Ineichen P, Seals R. Modelling daylight availability and irradiance components from direct and global irradiance. *Solar Energy* 1990; 44(5): 271–289. [http://dx.doi.org/10.1016/0038-092X\(90\)90055-H](http://dx.doi.org/10.1016/0038-092X(90)90055-H)
- [16] Elminir K H, Ghitas AE., El-Hussainy F., Hamid R., Beheary MM, Abdel-Moneim KM. Optimum solar flat-plate collector slope: Case study for Helwan, Egypt. *Energy Conversion and Management* 2006; 47 (5): 624–637. <http://dx.doi.org/10.1016/j.enconman.2005.05.015>
- [17] Patek J, Klomfar J. Computationally effective formulation of the thermodynamic properties of LiBr-H₂O solution from 273 to 500K over full composition range. *International Journal of Refrigeration* 2006; 29 (4): 566-578. <http://dx.doi.org/10.1016/j.ijrefrig.2005.10.007>
- [18] Patek J, Klomfar J. A simple formulation for thermodynamic properties of steam from 273 to 523 K, explicit in temperature and pressure. *International Journal of Refrigeration* 2009; 32 (5): 1123-1125, 2009. <http://dx.doi.org/10.1016/j.ijrefrig.2008.12.010>
- [19] J.T. Kotas, *The exergy method of thermal plant Analysis*. Lavoisier: Paris, 1987.
- [20] A. Bejan, G. Tsatsaronis G and M. Moran M. *Thermal design and optimization*. Wiley: New York, 1996.
- [21] Ortega O, Garcia O, Best R, Gomez VH. Two-phase flow modeling of a solar concentrator applied as ammonia vapor generator in an absorption refrigerator. *Renewable Energy* 2008;33(9):2064–2076. <http://dx.doi.org/10.1016/j.renene.2007.11.016>

Nomenclature

A_C	Collector surface area, m ²
COP	Thermal efficiency (coefficient of performance) of the absorption cooling system
C_p	Specific heat of water, kJ/kg.K
Ex	Exergy, kW
F'	Collector efficiency factor.
F_R	Collector heat removal factor
H	Enthalpy, kJ/kg
HPG	High pressure generator
I_G	Instantaneous solar radiation incident, kW/m ²
LPG	Low pressure generator
M	Mass flow rate of the fluid stream,
Q	Heat (Energy), kW
S	Entropy, kJ/kg.K
T	Temperature, K
U_L	collector overall loss coefficient, kW/m ² .K
W	Mechanical work transfer to or from the system, kW
T	Temperature of the jet, K

Greek Symbols

η	Efficiency
$(\tau.\alpha)$	is the transmittance-absorptance products

Subscripts

0	Reference value
A	Ambient
Aux	Auxiliary
B	Cold source
Cd	Condenser
D	Destruction
Ev	Evaporator
Fi	The fluid at the inlet to the collector.
FPC	Flat plate collectors
G	Generator
gH	High pressure generator
gL	Low pressure generator
H	Hot source
P	Pump
Th	Thermal
U	Useful